Prediction of autoignition-stabilized flame dynamics in a backward-facing step reheat combustor configuration

Symposium on Thermoacoustics in Combustion: Industry meets Academia (SoTiC 2023)
Sept. 11 - Sept. 14, 2023
Zurich, Switzerland
Paper No.: XXX

Harish S. Gopalakrishnan[1], Tarjei Heggset[2], Andrea Gruber[2, 3], Mirko R. Bothien[1] and Jonas Moeck[3]

Keywords
Combustion instability, autoignition-stabilized flames, reheat combustor, flame response

Abstract

Hydrogen combustion in a sequential combustor with a propagation-stabilized flame in the first stage and an autoignition-stabilized flame in the second reheat stage offers fuel flexible and efficient power generation with minimal greenhouse gas emissions. However, unsteady thermoacoustic phenomena driven by the interactions between the flame dynamics and the combustor acoustics can result in large amplitude heat release rate and pressure oscillations, which can cause hardware damage and performance losses. A key component required to understand and predict thermoacoustic oscillations in reheat combustors is the knowledge of the response of the autoignition-stabilized flame to unsteady acoustic and convective disturbances. In this paper, we extend a simplified particle based framework, originally proposed for computing the flame response in a simple one-dimensional reheat combustor configuration (Gopalakrishnan et al. 2021), to a two-dimensional backward-facing step geometry. The present particle based framework treats the flow as a collection of independent Lagrangian fluid elements which evolve in time. The temperature evolution of each fluid particle is computed by integrating the momentum, energy and species mass balance equations for that particle in time. The unsteady heat release rate and instantaneous flame position are then computed by stitching together the particle evolution data. The predictions of the flame response framework are thereafter compared with fully compressible Large eddy simulations (LES) of a reheat flame forced by acoustic and entropy disturbances. The flame response predictions obtained from the present approach match well with the LES data, suggesting that the present particle based framework can be used to compute flame transfer functions of reheat flames and consequently give insight into the thermoacoustic stability characteristics of reheat combustors.

Introduction

Power generation in land based gas turbines using hydrogen as a fuel is gaining interest and popularity due to the reduced pollutant emissions. However, conventional single-stage combustors with propagation-stabilized flames face challenges in burning highly reactive fuels such as hydrogen efficiently. This is because the high reactivity of hydrogen results in an increased flashback tendency. In principle, a reduction in flame temperature could mitigate this, but undesirable performance penalties would result. A promising alternative is to use a two-stage sequential combustor architecture with a propagation-stabilized flame in the first stage and an autoignition-stabilized flame in the second, reheat stage (Pennell et al. 2017; Bothien et al. 2019b,c; Ciani et al. 2020). In the reheat stage of a sequential burner, a vitiated mixture of a highly reactive fuel, by virtue of its high temperature and pressure, autoignites and burns within a reaction front where the combustion process is predominantly controlled by spontaneous ignition.

Thermoacoustic instability, which is caused due to the interaction between flame dynamics and the acoustic modes of the combustor, results in self-sustained pressure and heat release oscillations which severely affect the operation of all combustion systems (Lieuwen and Yang 2005). Since flames are acoustically active elements, any acoustic disturbance can modulate the heat release rate of the flame over one cycle of oscillation. In propagation-stabilized flames, an acoustic disturbance can create a heat release rate oscillation by either modulations in flame area (Boyer and Quinard 1990; Schuller et al. 2003; Preetham et al. 2008), or by forcing the fuel injection system leading to convected equivalence ratio fluctuations (Lieuwen et al. 2001; Schuermans et al. 2003; Shreekrishna et al. 2010), or by exciting vortical structures which wrinkle the flame and create flame area oscillations (Poinsot et al. 1987; Hemchandra et al. 2018; Oberleithner et al. 2011; Moeck et al. 2012). These unsteady integrated heat release rate oscillations associated with the flame act as a monopole source of sound (Strahle 1971)

[1]Zürich University of Applied Sciences, Institute of Energy Systems and Fluid-Engineering, Winterthur, Switzerland
[2]SINTEF Energy Research, Trondheim, Norway
[3]Department of Energy and Process Engineering, Norwegian University of Science and Technology, Trondheim, Norway

Corresponding author:
Harish Gopalakrishnan, Zürich University of Applied Sciences, Institute of Energy Systems and Fluid-Engineering, Technikumstrasse 9, Winterthur 8401, Switzerland.
Email: gopa@zhaw.ch

generating acoustic disturbances which in turn perturb the flame. Under certain conditions this process can be self-amplifying and lead to an instability.

Autoignition-stabilized flames are governed by the balance between convective and chemical processes. More specifically, the stabilization of an autoignition front is dictated by the balance between the flow residence time and the mixture ignition time. In view of this fact, finite Mach numbers (in the range of $0.2 - 0.3$) are often required to stabilize these flames in reheat burners. At these conditions, the normalized pressure and temperature fluctuations induced by an acoustic wave are comparable to the velocity fluctuations. Consequently, a key mechanism leading to self-sustained oscillations in reheat combustors can be attributed to the modulation of the ignition chemistry of the reactant mixture by the acoustic temperature and pressure oscillations, which result in oscillations in the flame front location and heat release rate (Gant et al. 2020; Gopalakrishnan et al. 2021).

Recent studies (Bothien et al. 2019a; Gruber et al. 2021) conducted large eddy simulations (LES) and direct numerical simulations (DNS) of autoignition fronts in simple geometrical configurations and showed that autoignition fronts are highly sensitive to temperature fluctuations induced by acoustic disturbances and exhibit, under special conditions, unstable self-sustained thermoacoustic oscillations. Thermoacoustic instability linked to autoignition flame front dynamics was also observed in a laboratory-scale sequential combustor by Noiray and co-workers (Schulz et al. 2019). A variety of instability mechanisms can cause self-sustained oscillations in reheat combustors. First, entropy waves, which are temperature fluctuations generated by the first-stage flame, convect downstream and result in flame position and heat release rate fluctuations of the reheat flame (Bothien et al. 2019a; Gant et al. 2019, 2020). Second, the upstream-traveling acoustic disturbance generated by the unsteady autoignition front also modulates the ignition chemistry of the upstream unburnt reactant mixture resulting in flame front oscillations (Gopalakrishnan et al. 2023a,b). Both these mechanisms have been investigated extensively in the framework of a one-dimensional reheat combustor configuration in the aforementioned works.

An important component to understand and predict thermoacoustic instability in combustors is the knowledge of the response of the flame to acoustic and convective disturbances. While detailed numerical computations and experiments can be used to obtain the flame response, they are expensive and time-consuming. Thus, one usually resorts to physics-based simplified frameworks to obtain the flame response over the extensive parameter space. One such example is the G-equation based framework to compute the response of propagation-stabilized flames to velocity and equivalence ratio disturbances (Fleifil et al. 1996; Schuller et al. 2003; Preetham et al. 2008). In such a framework, the propagating flame is described as a thin surface $(G = 0)$ which separates reactants $(G < 0)$ and products $(G > 0)$. A transport equation is then derived for the G field which, when solved using suitable methods, yields the flame front kinematics and heat release dynamics. With regards to autoignition-stabilized flames, simplified models to describe the flame dynamics were based on a slightly different approach. Since autoignition fronts are predominantly controlled by the interplay of convective and chemical kinetic mechanisms, these flames are conveniently described by the evolution of a series of non-interacting reactive fluid parcels. In other words, the flow was treated as a collection of fluid particles whose temperature, pressure and velocity are modulated by both the acoustic disturbances and the chemical reactions. Such an approach formed the basis for computing the autoignition-stabilized flame dynamics in the prior works of Zellhuber et al. (2014), Gant et al. (2020) and Gopalakrishnan et al. (2021). This particle based Lagrangian approach was also validated with detailed flow computations in these works.

Practical reheat combustors contain flames which are stabilized both by propagation and autoignition. Consider, for example, the Ansaldo Energia GT36 gas turbine engine (Pennell et al. 2017). Majority of prior works get insight into the flame dynamics in this configuration by modeling the reheat stage of the sequential burner as a backward-facing step geometry (Yang et al. 2015; Scarpato et al. 2016; Schulz and Noiray 2018, 2019; Konduri et al. 2019; Bothien et al. 2019a). In such a geometry, part of the flame stabilization occurs due to flame propagation mechanism assisted by the recirculation zone formed downstream of the step, while part of the flame stabilization occurs due to autoignition. Indeed, the work of Schulz and Noiray (2019) showed that three regimes of flame-stabilization are possible even in a geometry as simplistic as a one-dimensional duct. This was concluded by computing a wide range of 1D flame solutions in Cantera (Goodwin et al. 2018) and plotting these solutions in a parameter space of u_{in}/S_l and $\tau_{\text{res}}/\tau_{AI}$, where u_{in} and S_l are the inlet mixture velocity and laminar consumption speed, and τ_{res} and τ_{AI} are the residence time and ignition time of the reactant mixture, respectively. The three regimes of flame stabilization observed in their work (propagation, propagation assisted by autoignition and autoignition) were also observed in the backward-facing step combustor geometry as well.

Given the fact that flames in practical reheat combustion systems are stabilized both by propagation and autoignition, there arises a need for us to develop a simplified model which can predict the flame dynamics of this composite flame. In this regard, an important question that needs to be answered is: even in conditions wherein a two-dimensional reheat flame is predominantly stabilized by autoignition (see, for example, Bothien et al. (2019a) and Schulz and Noiray (2019)), how do the Lagrangian based models originally proposed for a one-dimensional front in prior papers (Zellhuber et al. 2011; Gant et al. 2020; Gopalakrishnan et al. 2021) perform ?

The main objective of the present paper is to extend the Lagrangian particle based framework proposed in Gopalakrishnan et al. (2021) to compute the dynamics of autoignition-stabilized flames in a more realistic two-dimensional backward-facing step reheat combustor. This flow consists of a vitiated hydrogen–air reactant mixture entering the combustor at a sufficiently high temperature and pressure such that this mixture spontaneously ignites downstream and results in an autoignition front. To study flame dynamics, the

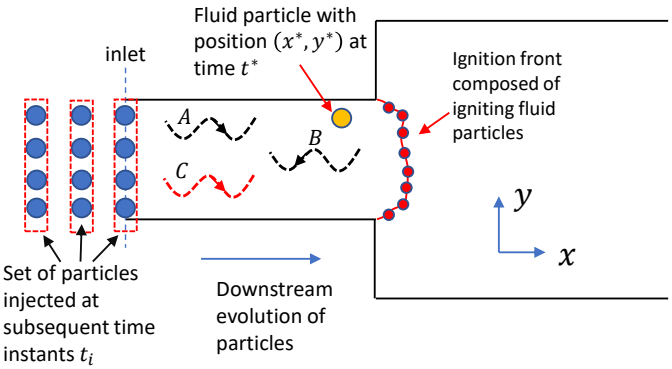

Figure 1. Schematic of the combustor geometry with the imposed disturbances and the particle injection scheme.

combustor inlet is forced by downstream traveling acoustic and entropy disturbances. The predictions of the flame response framework are compared with LES computations to establish its validity.

Flame response framework and LES computations

In this section, the flame response framework and the LES computations used to validate the flame response predictions are described. As discussed previously, the geometrical configuration considered for the computations is a simplified model representation of a realistic reheat combustor. This model consists of a backward-facing step combustor through which a hydrogen–air reactant mixture enters at high temperature and pressure (Figure 1). Owing to the high temperature of the reactants, chemical reactions are already initiated at the combustor inlet, and the reactant mixture spontaneously ignites at a downstream location resulting in the formation of a stabilized autoignition front. The location of the autoignition-stabilized flame in the combustor is governed by the balance between residence time and mixture ignition time. This flow is also forced at the inlet by downstream-traveling acoustic and entropy disturbances (waves A and C in Figure 1). In addition to these disturbances, the ignition front generates an upstream-traveling acoustic disturbance (wave B in Figure 1), which also modulates the incoming reactant mixture. The combustor geometry is essentially two-dimensional with a mixing duct of length 0.03 m and with a transverse dimension of 0.01 m. This is followed by an area expansion with an expansion ratio of 2 and a combustion chamber of length 0.06 m. The dimensions of the backward-facing step configuration are chosen such that the length of the mixing duct matches closely with the mean ignition location of the autoignitive mixture. This ensures that the flame is stabilized just downstream of the step.

To validate the flame response framework proposed in this work, we carry out compressible forced LES computations wherein the inlet of the combustor is forced by small amplitude acoustic and convective entropy disturbances. The Navier–Stokes equations are solved within the framework of the open source code OpenFOAM (Weller et al. 1998). The partially-stirred reactor (PaSR) turbulent combustion model is used for the LES computations. The mean flow parameters and the species mass fractions used correspond to typical inlet conditions of a realistic reheat combustor. The reader is referred to our prior paper (Gopalakrishnan et al. 2021) for these values. All the combustor walls are maintained as no-slip with a specified fixed temperature of 750 K. The LES computations are performed at three different forcing frequencies namely 100 Hz, 500 Hz and 1000 Hz.

To compute the flame response to the imposed disturbances, the reacting flow is visualized as a series of non-interacting, independently evolving fluid particles. The flame response is computed at discrete time instants $t_i \in [0, \mathcal{T}]$, where $\mathcal{T}$ is the time period of the imposed acoustic/convective disturbances. At each time instant t_i, a number of fluid particles are injected across the combustor inlet plane (see Figure 1). The evolution of each fluid particle in Lagrangian time t^* is then computed by time integrating the governing equations for each particle. It is important to note that t^* is a fictitious local time assigned to each particle for the purpose of tracking that particle. For any given particle, $t^* = 0$ at the instant this particle is injected at the combustor inlet. t^* is different from the physical global time t. If t_i is the time at which a particle is injected at the combustor inlet, the relation between global time and particle time is given by $t = t_i + t^*$.

The change in temperature (ΔT) of a fluid particle over a small time interval of Δt^* is a combination of the temperature change due to chemical reactions (ΔT_c) and the temperature change due to acoustic and entropy disturbances (ΔT_d). Thus, we can write

$$\Delta T = \Delta T_c + \Delta T_d. \tag{1}$$

The above equation can be written in terms of derivatives assuming that $\Delta t^* \to 0$:

$$\frac{DT}{Dt^*} = \frac{DT_c}{Dt^*} + \frac{DT_d}{Dt^*}. \tag{2}$$

The first term in the RHS of the above equation, which is the time rate of change of temperature of a fluid particle due to chemical reactions, is given by the Lagrangian form of the energy equation.

$$\rho C_p \frac{DT_c}{Dt^*} = \dot{\omega}_h(T, p, Y_i) + \frac{\partial}{\partial x}\left(\lambda \frac{\partial T}{\partial x}\right) + \frac{\partial}{\partial y}\left(\lambda \frac{\partial T}{\partial y}\right), \tag{3}$$

where ρ, T, p, Y_i denote the density, temperature, pressure and species mass fractions associated with the fluid particle, respectively. C_p represents the specific heat at constant pressure. The chemical heat release source term is represented by $\dot{\omega}_h$, λ is the thermal conductivity, and x, y are the axial and transverse spatial locations. In writing the above equation, it is implicitly assumed that the radiative heat flux, viscous heating and heat flux due to species diffusion terms are neglected. Prior works (Gant et al. 2020; Gopalakrishnan et al. 2021) which computed the autoignition front response by neglecting diffusive effects showed, by comparison with detailed DNS computations, that excellent predictions of the ignition front heat release response can be obtained even without accounting for diffusive terms. The heat conduction term has to be included in the present geometry because the reheat combustor walls are maintained at a lower temperature (750 K) compared to the reactant temperature (1060 K) and, thus, there can be significant heat transfer due to conduction close to the walls.

One important aspect to note in Equation (3) is that all terms on the right hand side are temporally varying. Specifically, the heat conduction term is an unsteady quantity. However, it is crucial to realize that computation of this unsteady heat transfer term from a particle based approach is not straightforward. Since these terms involve axial and transverse spatial derivatives, computation of these derivatives for any given fluid particle requires the temperature data of not only that particle but also of all other particles in a small neighbourhood surrounding that particle. Since fluid particles lying in the transverse direction are convected with different mean velocities, the temperature data of all particles in a small neighbourhood around a particle is unknown at any time t^*. To overcome this difficulty, the heat conduction term in Equation (3) is assumed to be only spatially dependent (steady) and is obtained from the time-averaged temperature and the thermal conductivity fields. Thus, the energy equation is rewritten as:

$$\rho C_p \frac{DT_c}{Dt^*} = \dot{\omega}_h(T, p, Y_i) + q_x(x^*, y^*) + q_y(x^*, y^*), \tag{4}$$

where x^*, y^* are the axial and transverse co-ordinates of the particle at any time t^*, and q_x, q_y are derived from the time-averaged variables (λ_0, T_0) as

$$q_x = \frac{\partial}{\partial x}\left(\lambda_0 \frac{\partial T_0}{\partial x}\right), q_y = \frac{\partial}{\partial y}\left(\lambda_0 \frac{\partial T_0}{\partial y}\right). \tag{5}$$

Thus, the effect of heat transfer is taken into account by imposing a background heat conduction steady source term on top of the fluid particle evolution. The evolution equations for the species mass fractions of the reacting fluid particle and the particle position are given by (these equations help in calculating x^*, y^* and $\dot{\omega}_h$ terms in the energy equation)

$$\frac{DY_i}{Dt^*} = \frac{\mathrm{MW}_i \dot{\omega}_i}{\rho}, \tag{6}$$

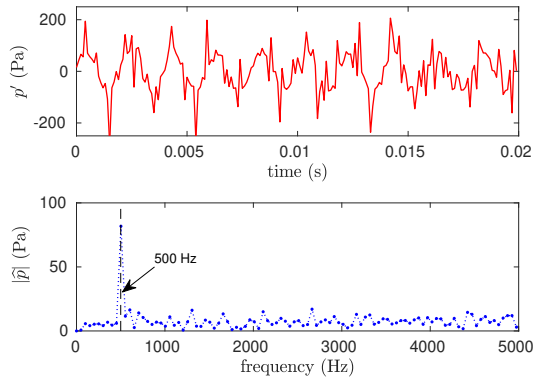

Figure 2. Pressure fluctuations at the inlet plane centerline as a function of time and the corresponding frequency spectrum. The flow is forced by acoustic and entropy waves at the inlet at a frequency of 500 Hz.

$$\frac{Dx^*}{Dt^*} = u(t^*), \frac{Dy^*}{Dt^*} = v(t^*), \tag{7}$$

where MW_i is the molecular weight of the i^{th} species, $\dot{\omega}_i$ is the production rate of the i^{th} species, and u, v are the particle velocities in the axial and transverse directions.

It is now apparent from Equations (4) and (7) that in order to integrate these equations, the instantaneous pressure and flow velocity has to be known at any spatial point (x^*, y^*) at time t^*. This is determined from the unsteady LES dataset. Any flow quantity (Φ) in the LES data is first decomposed into a mean and a fluctuating component as follows:

$$\Phi(x, y, t) = \Phi_0(x, y) + \widehat{\Phi}(x, y)e^{i\omega_f t} + \Phi_s(x, y, t), \tag{8}$$

where Φ_0 denotes the time-averaged mean value, $\widehat{\Phi}$ denotes the Fourier transform of the fluctuations at the forcing frequency ω_f, and Φ_s represents the stochastic turbulent fluctuations. The above decomposition is motivated by observation of the frequency spectra of the pressure fluctuations at any point in the combustor when forced harmonically, for example, in Figure 2. The pressure fluctuations show a strong Fourier component at the frequency of forcing in addition to a small broadband component. Since the primary interest here is to compute the linear response of the flame to harmonic acoustic/entropy forcing, the important component to consider in Equation (8) is the Fourier component at the forcing frequency. Figure 3 plots the mean and the Fourier decomposed fluctuation amplitude (at the forcing frequency ω_f) of the temperature and axial velocity component obtained from the LES data. The mean quantities show an autoignition front stabilized close to the step location. The ignition front creates a region of high velocity due to gas expansion. One important aspect should be clarified in this figure. It can be seen that the Fourier decomposed temperature and velocity oscillations reach very high values locally near the mean ignition front location ($x = 0.033$ m). This is due to the fact that the autoignition front exhibits harmonic oscillations in its position in response to the imposed disturbances. Due to the ignition front position fluctuations and because the temperature and velocity increase drastically across

the ignition front, we see a large amplitude fluctuation region close to the ignition front. The amplitude of the imposed disturbances is still quite small (around 0.7% of the respective mean values) to ensure a linear flame response.

The fluctuating flow quantities in the region upstream of the autoignition front can be obtained by performing a wave decomposition at the combustor inlet to determine the acoustic and entropy wave amplitudes. The primitive variable fluctuations can then be determined using a wave ansatz. The mean and Fourier transform of any primitive variable (Φ) is first averaged over the inlet to determine an 'effective' inlet value (Φ^e) of that quantity:

$$\begin{aligned} \Phi_0^e &= \frac{\int_{\text{inlet}} \Phi_0 dy}{\int_{\text{inlet}} dy}, \\ \widehat{\Phi}^e &= \frac{\int_{\text{inlet}} \widehat{\Phi} dy}{\int_{\text{inlet}} dy}. \end{aligned} \tag{9}$$

This is done because these quantities typically vary over the inlet cross section. The Fourier amplitudes of the pressure and density fluctuations associated with the acoustic (A, B) and entropy waves (C) at the inlet can be written as

$$\begin{aligned} \widehat{p}_A &= \frac{\widehat{p}^e + \rho_0^e c_0^e \widehat{u}^e}{2}, \\ \widehat{p}_B &= \frac{\widehat{p}^e - \rho_0^e c_0^e \widehat{u}^e}{2}, \\ \widehat{\rho}_C &= \widehat{\rho}^e - \frac{\widehat{p}^e}{(c_0^e)^2}, \end{aligned} \tag{10}$$

where c denotes the speed of sound.

From the amplitudes of the acoustic and entropy waves at the inlet, the primitive variable fluctuations at any point in the region upstream of the autoignition front can be written assuming one-dimensional propagation of these waves. The density fluctuation is written below as an example:

$$\begin{aligned} \rho'(x,y,t) = \frac{\widehat{p}_A}{(c_0^e)^2} e^{i\omega_f t} e^{-ik_A x} + \frac{\widehat{p}_B}{(c_0^e)^2} e^{i\omega_f t} e^{ik_B x} \\ + \widehat{\rho}_C e^{i\omega_f t} e^{-ik_C x}, \end{aligned} \tag{11}$$

where k denotes the wavenumber of the waves, whose expressions can be found in literature (Dowling 1995). The temperature (T'), velocity (u', v') and pressure fluctuations (p') can also be written in a similar manner (Dowling 1995; Gopalakrishnan et al. 2021). The wave ansatz form of the flow field fluctuations together with the mean fields will completely determine the instantaneous velocity and pressure experienced by the fluid particle at time t^*. As an example, the instantaneous velocity of a fluid particle at time t^* is given by

$$u(t^*) = u_0(x^*, y^*) + u'(x^*, y^*, t^* + t_i). \tag{12}$$

Similarly, the temperature fluctuations experienced by the fluid particle at time t^* can be written as

$$T_d(t^*) = T'(x^*, y^*, t^* + t_i). \tag{13}$$

Thus, knowing the mean values of all the primitive variables and the Fourier decomposed fluctuations of the primitive variables at the inlet from the LES data will allow us to construct all the terms in the evolution equations (4), (6), (7). The energy and species equations source terms are evaluated using the detailed chemical mechanism proposed by Li et al. (2004). The time integration of the evolution equations of a fluid particle are performed using stiff ode solver routines available in MATLAB.

Integration of the evolution equations for a particle injected at the combustor inlet at time t_i yields the particle temperature, species mass fractions and position as a function of the Lagrangian time t^*. From this data the ignition time (τ) of this particle can be determined as the time at which dT/dt^* is maximum. The ignition location $(x_{\text{ig}}, y_{\text{ig}})$ of this particle can be determined as

$$\begin{aligned} x_{\text{ig}}(t_i + \tau) &= x^*(\tau), \\ y_{\text{ig}}(t_i + \tau) &= y^*(\tau). \end{aligned} \tag{14}$$

Repeating this process by injecting particles at the inlet over different time instants t_i allows us to construct the co-ordinates of the ignition front at different instants of time. The ignition front co-ordinates $(X_{\text{ig}}, Y_{\text{ig}})$ at any time t are obtained as the curve that smoothly connects all fluid particles which ignite at that instant.

The integrated heat release rate response of the flame at any time instant can be computed as

$$\dot{Q}(t) = \int_C \rho \Delta h_c (\mathbf{v} - \mathbf{V}_{\text{ig}}).\mathbf{n}\, ds, \tag{15}$$

where the line integral is performed along the ignition front surface. In the above expression, Δh_c is the heat of reaction of the reactant mixture, $\mathbf{v}$ is the flow velocity vector, $\mathbf{V}_{\text{ig}}$ is the ignition front velocity vector given by $(dX_{\text{ig}}/dt)\vec{i} + (dY_{\text{ig}}/dt)\vec{j}$, and $\mathbf{n}$ is the unit normal vector to the flame.

Results and Discussion

Figure 4 shows a typical result from the forced LES computations, where the fluctuations in temperature at the combustor inlet in terms of the acoustic and entropy wave amplitudes are shown. The amplitudes of the imposed waves are maintained sufficiently small to capture the linear flame response. The right plot in Figure 4 shows the integrated heat release rate in the domain. It can be seen that even though the forcing is imposed at 500 Hz, the heat release response does not happen purely at this frequency. Higher frequency components are superimposed on top of the response at the forcing frequency. However, in this work we focus purely on the response of the ignition front at the imposed forcing frequency. Thus, the heat release response is Fourier-decomposed at the forcing frequency for the purpose of comparison with the Lagrangian framework.

Figures 5 and 6 show the results obtained from the flame response framework in terms of the instantaneous ignition front shape at different time instants. The ignition front is stabilized close to the step and exhibits small amplitude fluctuations in its position in response to the imposed forcing. Two flame response computations are carried out. In the first computation, the heat conduction term (last two terms in the RHS of Equation (4)) are neglected, while in the second computation the heat conduction term is taken into account. Figure 6 reveals that in both these computations, the flame response framework is able to predict, to reasonable

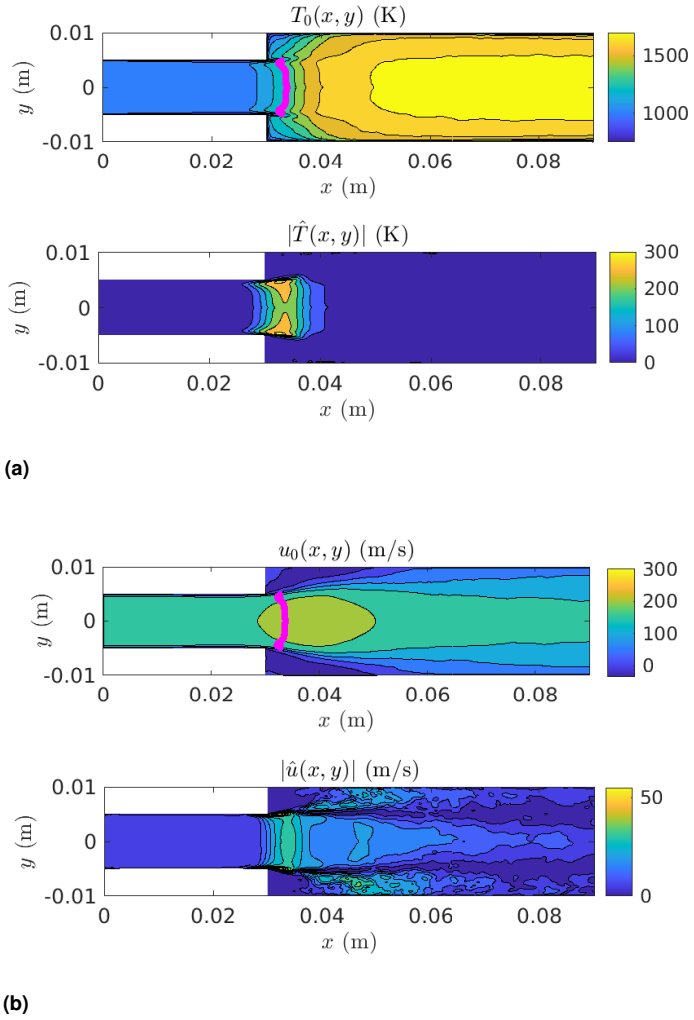

Figure 3. Mean and Fourier decomposed fluctuation amplitude corresponding to the (a) temperature and (b) axial velocity fields obtained from the LES data. The magenta solid line in the mean plots denotes the time-averaged autoignition front.

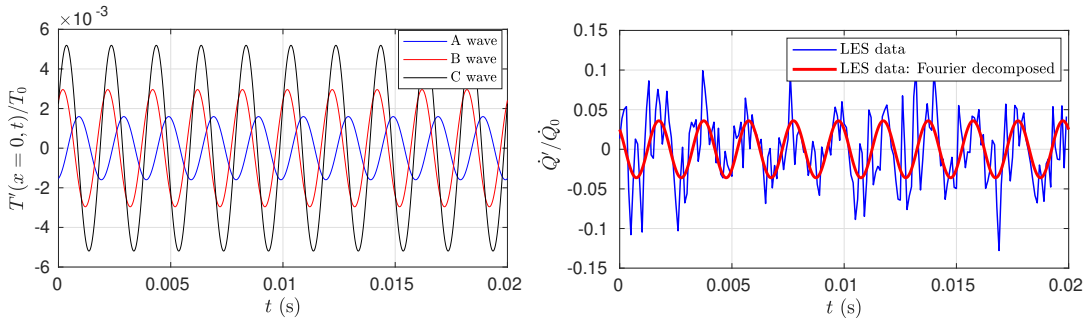

Figure 4. Typical result from the LES computation showing the temperature fluctuations at the inlet due to the acoustic and entropy waves propagating upstream of the autoignition front. The right plot shows the normalized global (area) integrated heat release rate in the combustor domain. The forcing frequency is 500 Hz.

accuracy, the ignition front shape. It is evident that when the heat transfer terms are neglected, the shape of the ignition front close to the walls is not accurately predicted. This is to be expected as we expect the effect of the heat transfer terms to be significant and important near the walls. In any case, the Lagrangian flame response framework performs well in predicting the ignition front dynamics.

The heat release rate response of the autoignition front is shown in Figure 7. The results are shown for three different frequencies. First, we observe that the present flame response framework is able to predict, with good accuracy, the integrated heat release rate dynamics. Second, we observe that incorporating the influence of heat transfer does not significantly change the predictions. Third, we observe that the gain of the heat release rate response transfer function increases with increase in frequency. This observation was previously observed for one-dimensional autoignition fronts as well in Gant et al. (2020) and Gopalakrishnan et al. (2021). One reason for this behaviour is because of the term $\mathbf{V}_{\mathrm{ig}}$ in the expression for heat release rate (Equation (15)).

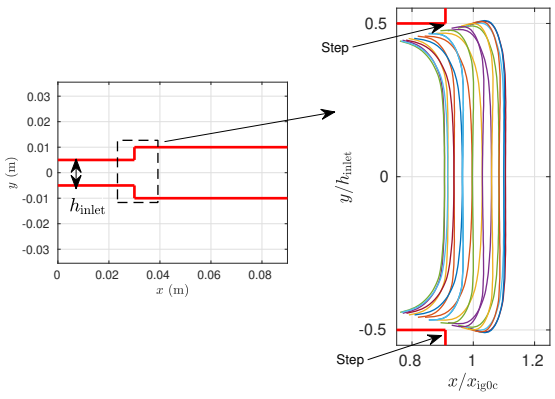

Figure 5. Typical result from the flame response computation showing the ignition front at different instants of time over one forcing cycle. The left plot shows the backward-facing step combustor geometry, and the right plot shows the ignition front at different time instants. In the right plot, the x-axis is normalized by the mean ignition location of the particle at the centerline to show the amplitude of normalized fluctuations in the ignition front position, while the y-axis is normalized by the channel inlet width to show the spatial extent of the ignition front.

For a given ignition front oscillation amplitude, the $\mathbf{V}_{\text{ig}}$ fluctuations increases with an increase in frequency as it involves a derivative with respect to time.

Conclusion

In this paper, a Lagrangian particle based simplified framework was developed to compute the autoignition-stabilized flame dynamics in a two-dimensional backward-facing step reheat combustor configuration. Understanding the flame front dynamics is an important aspect to get insight into the thermoacoustic behaviour of reheat combustors. The Lagrangian framework works by injecting a series of reacting fluid particles at the inlet of the combustor. These particles are evolved in time by integrating the energy, species and momentum equations. The framework uses as inputs the mean flow quantities and Fourier decomposed velocity and pressure oscillations at the combustor inlet extracted from a CFD computation. In the present paper, we also carried out reactive LES computations in which the combustor is forced at the inlet. The predictions of the framework agreed very well with the LES data both in terms of the ignition front position dynamics and the global heat release dynamics. This suggests that simplified frameworks such as the one proposed in the present paper can be used to compute flame response transfer functions to assess the thermoacoustic instability of a combustion system involving autoignition-stabilized flames.

Acknowledgments

This publication has been produced with support from the NCCS Centre, performed under the Norwegian research program Centres for Environment-friendly Energy Research (FME). This project has received funding from the the Research Council of Norway under the Reheat2H2 project (project number 295203).

References

Bothien M, Lauper D, Yang Y and Scarpato A (2019a) Reconstruction and analysis of the acoustic transfer matrix of a reheat flame from large-eddy simulations. *Journal of Engineering for Gas Turbines and Power* 141(2).

Bothien MR, Ciani A, Wood JP and Fruechtel G (2019b) Sequential combustion in gas turbines: the key technology for burning high hydrogen contents with low emissions. In: *Turbo Expo: Power for Land, Sea, and Air*, volume 58615. American Society of Mechanical Engineers, p. V04AT04A046.

Bothien MR, Ciani A, Wood JP and Fruechtel G (2019c) Toward decarbonized power generation with gas turbines by using sequential combustion for burning hydrogen. *Journal of Engineering for Gas Turbines and Power* 141(12).

Boyer L and Quinard J (1990) On the dynamics of anchored flames. *Combustion and flame* 82(1): 51–65.

Ciani A, Wood JP, Wickström A, Rørtveit GJ, Steeneveldt R, Pettersen J, Wortmann N and Bothien MR (2020) Sequential combustion in Ansaldo Energia gas turbines: The technology enabler for CO2-free, highly efficient power production based on hydrogen. In: *Turbo Expo: Power for Land, Sea, and Air*, volume 84126. American Society of Mechanical Engineers, p. V04AT04A041.

Dowling AP (1995) The calculation of thermoacoustic oscillations. *Journal of Sound and Vibration* 180(4): 557–581.

Fleifil M, Annaswamy A, Ghoneim Z and Ghoniem A (1996) Response of a laminar premixed flame to flow oscillations: A kinematic model and thermoacoustic instability results. *Combustion and Flame* 106(4): 487–510.

Gant F, Gruber A and Bothien MR (2020) Development and validation study of a 1D analytical model for the response of reheat flames to entropy waves. *Combustion and Flame* 222: 305–316.

Gant F, Scarpato A and Bothien MR (2019) Occurrence of multiple flame fronts in reheat combustors. *Combustion and Flame* 205: 220–230.

Goodwin DG, Speth RL, Moffat HK and Weber BW (2018) Cantera: An object-oriented software toolkit for chemical kinetics, thermodynamics, and transport processes. https://www.cantera.org. Version 2.4.0.

Gopalakrishnan HS, Gruber A and Moeck J (2021) Response of auto-ignition-stabilized flames to one-dimensional disturbances: Intrinsic response. *Journal of Engineering for Gas Turbines and Power* 143(12): 121011.

Gopalakrishnan HS, Gruber A and Moeck J (2023a) Computation of intrinsic instability and sound generation from auto-ignition fronts. *Journal of Engineering for Gas Turbines and Power* 145(4): 041008.

Gopalakrishnan HS, Gruber A and Moeck JP (2023b) Computation and prediction of intrinsic thermoacoustic oscillations associated with autoignition fronts. *Combustion and Flame* 254: 112844.

Gruber A, Bothien MR, Ciani A, Aditya K, Chen JH and Williams FA (2021) Direct numerical simulation of hydrogen combustion at auto-ignitive conditions: Ignition, stability and turbulent reaction-front velocity. *Combustion and Flame* 229: 111385.

Hemchandra S, Shanbhogue S, Hong S and Ghoniem AF (2018) Role of hydrodynamic shear layer stability in driving

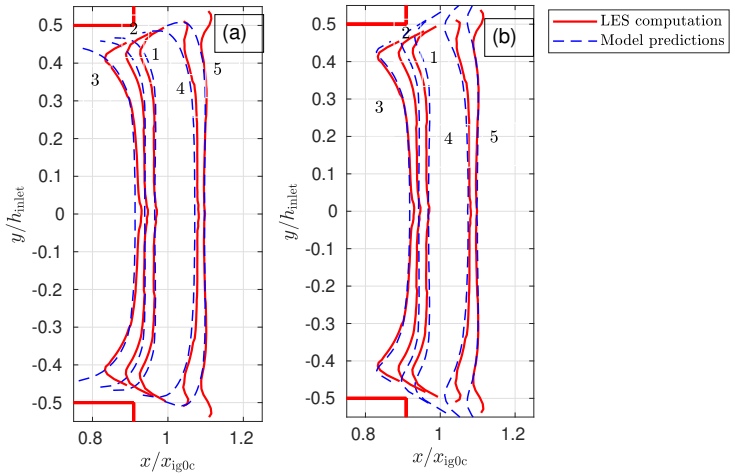

Figure 6. Comparison of the ignition front shape obtained from the LES computations at different instants of time over one forcing cycle with the predictions of the flame response framework for the case where the heat conduction terms are neglected (a), and the case where the heat conduction terms are considered (b). The time instants $1, 2, 3, 4, 5$ correspond to the forcing cycle phase of $0°, 20°, 90°, 190°, 270°$, respectively. The forcing frequency is 500 Hz.

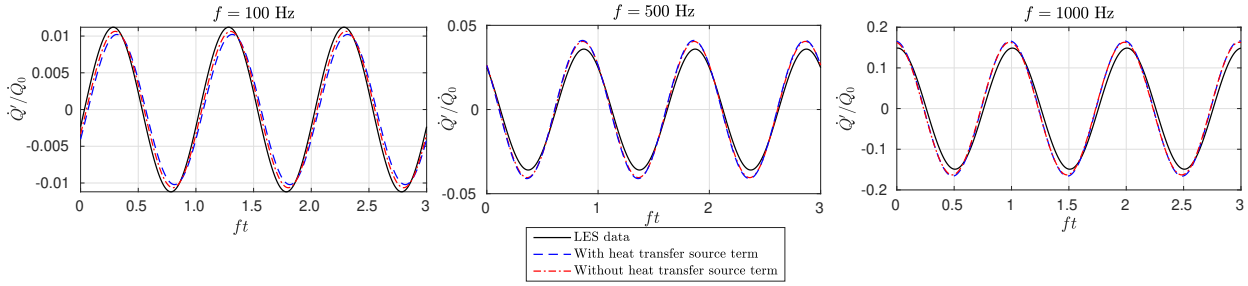

Figure 7. Heat release rate response of the ignition front compared with the globally integrated heat release rate obtained from the LES data.

combustion instability in a premixed propane-air backward-facing step combustor. *Physical Review Fluids* 3(6): 063201.

Konduri A, Gruber A, Xu C, Lu T, Krisman A, Bothien MR and Chen JH (2019) Direct numerical simulation of flame stabilization assisted by autoignition in a reheat gas turbine combustor. *Proceedings of the Combustion Institute* 37(2): 2635–2642.

Li J, Zhao Z, Kazakov A and Dryer FL (2004) An updated comprehensive kinetic model of hydrogen combustion. *International Journal of Chemical Kinetics* 36(10): 566–575.

Lieuwen T, Torres H, Johnson C and Zinn B (2001) A mechanism of combustion instability in lean premixed gas turbine combustors. *J. Eng. Gas Turbines Power* 123(1): 182–189.

Lieuwen TC and Yang V (2005) *Combustion instabilities in gas turbine engines: operational experience, fundamental mechanisms, and modeling*. Vol 210 of Progress in Astronautics and Aeronautics, American Institute of Aeronautics and Astronautics, Reston, Virginia.

Moeck JP, Bourgouin JF, Durox D, Schuller T and Candel S (2012) Nonlinear interaction between a precessing vortex core and acoustic oscillations in a turbulent swirling flame. *Combustion and Flame* 159(8): 2650–2668.

Oberleithner K, Sieber M, Nayeri C, Paschereit C, Petz C, Hege HC, Noack B and Wygnanski I (2011) Three-dimensional coherent structures in a swirling jet undergoing vortex breakdown: stability analysis and empirical mode construction. *Journal of Fluid Mechanics* 679: 383–414.

Pennell DA, Bothien MR, Ciani A, Granet V, Singla G, Thorpe S, Wickstroem A, Oumejjoud K and Yaquinto M (2017) An introduction to the ansaldo GT36 constant pressure sequential combustor. In: *Turbo Expo: Power for Land, Sea, and Air*, volume 50855. American Society of Mechanical Engineers, p. V04BT04A043.

Poinsot TJ, Trouve AC, Veynante DP, Candel SM and Esposito EJ (1987) Vortex-driven acoustically coupled combustion instabilities. *Journal of fluid mechanics* 177: 265–292.

Preetham, Santosh H and Lieuwen T (2008) Dynamics of laminar premixed flames forced by harmonic velocity disturbances. *Journal of Propulsion and Power* 24(6): 1390–1402.

Scarpato A, Zander L, Kulkarni R and Schuermans B (2016) Identification of multi-parameter flame transfer function for a reheat combustor. In: *Turbo Expo: Power for Land, Sea, and Air*, volume 49767. American Society of Mechanical Engineers, p. V04BT04A038.

Schuermans B, Bellucci V and Paschereit CO (2003) Thermoacoustic modeling and control of multi burner combustion systems. In: *Turbo Expo: Power for Land, Sea, and Air*, volume 36851. pp. 509–519.

Schuller T, Durox D and Candel S (2003) A unified model for the prediction of laminar flame transfer functions: comparisons between conical and v-flame dynamics. *Combustion and Flame* 134(1): 21–34.

Schulz O, Doll U, Ebi D, Droujko J, Bourquard C and Noiray N (2019) Thermoacoustic instability in a sequential combustor: large eddy simulation and experiments. *Proceedings of the Combustion Institute* 37(4): 5325–5332.

Schulz O and Noiray N (2018) Autoignition flame dynamics in sequential combustors. *Combustion and Flame* 192: 86–100.

Schulz O and Noiray N (2019) Combustion regimes in sequential combustors: Flame propagation and autoignition at elevated temperature and pressure. *Combustion and Flame* 205: 253–268.

Shreekrishna, Hemchandra S and Lieuwen T (2010) Premixed flame response to equivalence ratio perturbations. *Combustion Theory and Modelling* 14(5): 681–714.

Strahle WC (1971) On combustion generated noise. *Journal of Fluid Mechanics* 49(2): 399–414.

Weller HG, Tabor G, Jasak H and Fureby C (1998) A tensorial approach to computational continuum mechanics using object-oriented techniques. *Computers in Physics* 12(6): 620–631.

Yang Y, Noiray N, Scarpato A, Schulz O, Düsing KM and Bothien M (2015) Numerical analysis of the dynamic flame response in alstom reheat combustion systems. In: *Turbo Expo: Power for Land, Sea, and Air*, volume 56680. American Society of Mechanical Engineers, p. V04AT04A048.

Zellhuber M, Bellucci V, Schuermans B and Polifke W (2011) Modelling the impact of acoustic pressure waves on auto-ignition flame dynamics. In: *Proceedings of the European Combustion Meeting, ECM*.

Zellhuber M, Schuermans B and Polifke W (2014) Impact of acoustic pressure on autoignition and heat release. *Combustion Theory and Modelling* 18(1): 1–31.